4. American Psychiatric Association, *Diagnostic and Statistical Manual of Mental Disorders, Version IV (DSM-IV)* (American Psychiatric Association, Washington, DC, 1994).
5. J. A. Parkinson, R. N. Cardinal, B. J. Everitt, *Prog. Brain Res.* **126**, 263 (2000).
6. B. J. Everitt *et al.*, *Ann. N.Y. Acad. Sci.* **877**, 412 (1999).
7. T. J. Bussey, B. J. Everitt, T. W. Robbins, *Behav. Neurosci.* **111**, 908 (1997).
8. B. W. Balleine, A. Dickinson, *Neuropharmacology* **37**, 407 (1998).
9. A. Bechara, H. Damasio, A. R. Damasio, G. P. Lee, *J. Neurosci.* **19**, 5473 (1999).
10. M. Ho, S. Mobini, T. Chiang, C. M. Bradshaw, E. Szabadi, *Psychopharmacology* **146**, 362 (1999).
11. J. Bizot, C. Le Bihan, A. J. Puech, M. Hamon, M. Thiébot, *Psychopharmacology* **146**, 400 (1999).
12. T. R. Wade, H. de Wit, J. B. Richards, *Psychopharmacology* **150**, 90 (2000).
13. R. N. Cardinal, T. W. Robbins, B. J. Everitt, *Psychopharmacology* **152**, 362 (2000).
14. M. Ernst, A. J. Zametkin, J. A. Matochik, P. H. Jons, R. M. Cohen, *J. Neurosci.* **18**, 5901 (1998).
15. G. Bush *et al.*, *Biol. Psychiatry* **45**, 1542 (1999).
16. K. Rubia *et al.*, *Am. J. Psychiatry* **156**, 891 (1999).
17. V. Russell, A. Devilliers, T. Sagvolden, M. Lamm, J. Taljaard, *Brain Res.* **676**, 343 (1995).
18. A. G. Sadile, *Neurosci. Biobehav. Rev.* **24**, 161 (2000).
19. J. L. Evenden, C. N. Ryan, *Psychopharmacology* **128**, 161 (1996).
20. Seventy-two naïve hooded Lister rats were housed under a reversed light-dark cycle and maintained at 90% of their free-feeding mass. All experimental procedures were subject to UK Home Office approval (Project Licence PPL 80/1324). To avoid the potential effects of the lesions on learning, we trained rats on the task preoperatively and then matched them to groups for surgery. The apparatus, training procedure, and task have been described elsewhere (*13*). Rats were trained and tested in chambers equipped with a 2.8-W houselight and two retractable levers on either side of a food alcove (fitted with a traylight LED) into which 45-mg sucrose pellets could be delivered. Rats were trained to respond for pellets on each lever under a schedule in which every lever-press delivered a pellet. Next, they were trained to make a nosepoke response in the alcove to gain access to a single lever, as described (*13*). Rats were then trained on the delay-of-reinforcement task (Fig. 1) with one session per day. Squads of 24 rats were trained for 19 sessions and then assigned to matched sham/lesion groups by ranking them according to a measure of their sensitivity to delay: the linear regression of percentage of choice of the large reinforcer versus log(delay + 1 s), calculated using data from the last three sessions. The ranked list was divided into pairs, and from each pair one rat was randomly assigned to the sham group and one to the lesion group. Group numbers at this point were 12 (ACC), 12 (ACC sham), 14 (AcbC), 10 (AcbC sham), 14 (mPFC), and 10 (mPFC sham).
21. Animals were anesthetized with Avertin and received excitotoxic lesions of the AcbC [anteroposterior (AP), mediolateral (ML), and dorsoventral (DV) coordinates: AP +1.2, ML ±1.8, DV –7.1 from bregma, 0.5 μl per site], ACC (AP +1.2, ML ± 0.5, DV –3.0 and –2.2; AP +0.5, ML ±0.5, DV –2.8 and –2.0; AP –0.2, ML ±0.5, DV –2.5 and –2.0 from bregma, 0.5 μl per site), or mPFC (AP +3.8, ML ±0.5, DV –1.5; AP +3.3, ML ±0.5, DV –3.0 and –1.5; AP +2.6, ML ±0.5, DV –1.5; anteroposterior and mediolateral coordinates from bregma, dorsoventral coordinate from dura, 0.5 μl per site), incisor bar at –3.3 mm (*37*), using 0.09 M quinolinic acid, which produces AcbC lesions that spare Acb shell neurons (*25*). Sham lesions were made in the same manner, except that vehicle was infused.
22. Rats were retested on the basic task for seven sessions to obtain a baseline of performance. Next, all delays were removed to establish whether the rats remained sensitive to the delays. Four sessions were given in which all delays were omitted in alternate sessions (counterbalanced across groups). Further behavioral tests included (i) repetition of the delay-omission test (three sessions with delays present and three sessions with no delays, counterbalanced); (ii) six further sessions with no delays, to establish rats' preference between the two reinforcers in a simple choice situation; and (iii) reintroduction of delays for a further six sessions. In the mPFC and AcbC experiments, locomotor activity was measured in wire cages equipped with infrared beams enabling movements to be registered. Rats were placed in these unfamiliar cages and activity was recorded for 2 hours. Finally, food consumption was measured in the home cage over 4 days. Rats were allowed free access to either 45-mg sucrose pellets or their maintenance chow for 30 min. The time taken to consume either 50 sucrose pellets or an equivalent mass of chow was recorded.
23. The statistical techniques used have been described elsewhere (*13*). Graphs show group means; error bars are ±1 SEM unless stated. Data were analyzed using analysis of variance (ANOVA); tests of significance were performed at $\alpha = 0.05$. For repeated-measures analyses, Mauchly's test of sphericity was applied and the degrees of freedom corrected using the Huynh-Feldt epsilon as appropriate. Where significant heterogeneity of variance was found, Mann-Whitney U tests were used instead of ANOVA for simple effects comparisons, whereas the Box correction was applied for between-group comparisons.
24. Rats were overdosed with pentobarbitone and perfused transcardially with phosphate-buffered saline and 4% paraformaldehyde. Their brains were removed, postfixed, cryoprotected in 20% sucrose, cut at 60 μm, stained with cresyl violet, and assessed. Nine rats were excluded as their lesions were inaccurate. Final group sizes were 9 (ACC), 12 (ACC sham), 11 (mPFC), 10 (mPFC sham), 10 (AcbC), and 10 (AcbC sham). For lesion schematics, see *Science* Online (www.sciencemag.org/cgi/content/full/1060818/DC1).
25. J. A. Parkinson, M. C. Olmstead, L. H. Burns, T. W. Robbins, B. J. Everitt, *J. Neurosci.* **19**, 2401 (1999).
26. E. M. Bowman, V. J. Brown, *Exp. Brain Res.* **123**, 439 (1998).
27. B. J. Cole, T. W. Robbins, *Behav. Brain Res.* **33**, 165 (1989).
28. A. Christakou, T. W. Robbins, B. J. Everitt, unpublished data.
29. W. Schultz, W. Tremblay, J. R. Hollerman, *Cereb. Cortex* **10**, 272 (2000).
30. J. C. Houk, J. L. Adams, A. G. Barto, in *Models of Information Processing in the Basal Ganglia*, J. C. Houk, J. L. Davis, D. G. Beiser, Eds. (MIT Press, Cambridge, MA, 1995), pp. 249–270.
31. J. D. Salamone, M. S. Cousins, S. Bucher, *Behav. Brain Res.* **65**, 221 (1994).
32. J. E. Aberman, J. D. Salamone, *Neuroscience* **92**, 545 (1999).
33. J. L. Muir, B. J. Everitt, T. W. Robbins, *Cereb. Cortex* **6**, 470 (1996).
34. A. Dietrich, J. D. Allen, *Behav. Neurosci.* **112**, 1043 (1998).
35. R. D. Rogers *et al.*, *J. Neurosci.* **19**, 9029 (1999).
36. G. E. Alexander, M. R. DeLong, P. L. Strick, *Annu. Rev. Neurosci.* **9**, 357 (1986).
37. G. Paxinos, C. Watson, *The Rat Brain in Stereotaxic Coordinates* (Academic Press, New York, ed. 4, 1998).

38. Supported by a Wellcome Trust programme grant and conducted within the Medical Research Council (MRC) Co-operative for Brain, Behaviour and Neuropsychiatry. Also supported by a UK MRC research studentship and an award from the University of Cambridge School of Clinical Medicine (R.N.C.). We thank C. H. Morrison and H. J. Sweet-Gossage for histological assistance.

19 March 2001; accepted 10 May 2001
Published online 24 May 2001;
10.1126/science.1060818
Include this information when citing this paper.

Conditional Restoration of Hippocampal Synaptic Potentiation in GluR-A–Deficient Mice

Volker Mack,[1] Nail Burnashev,[2]* Katharina M. M. Kaiser,[2] Andrei Rozov,[2] Vidar Jensen,[3] Øvind Hvalby,[3] Peter H. Seeburg,[1] Bert Sakmann,[2] Rolf Sprengel[1]†

Plasticity of mature hippocampal CA1 synapses is dependent on L-α-amino-3-hydroxy-5-methylisoxazole-4-propionate (AMPA) receptors containing the glutamate receptor A (GluR-A) subunit. In GluR-A–deficient mice, plasticity could be restored by controlled expression of green fluorescent protein (GFP)–tagged GluR-A, which contributes to channel formation and displayed the developmental redistribution of AMPA receptors in CA1 pyramidal neurons. Long-term potentiation (LTP) induced by pairing or tetanic stimulation was rescued in adult GluR-A$^{-/-}$ mice when ^{GFP}GluR-A expression was constitutive or induced in already fully developed pyramidal cells. This shows that GluR-A–independent forms of synaptic plasticity can mediate the establishment of mature hippocampal circuits that are prebuilt to express GluR-A–dependent LTP.

Of the four AMPA receptor subunits (GluR-A to GluR-D) constituting one family of glutamate-gated ion channels (*1–3*), GluR-A is essential for adult hippocampal LTP but not for spatial learning in a water maze task (*4*). Studies on mice lacking GluR-A provided evidence that after tetanic stimulation, increased transmission at Schaffer collateral (SC/CA1) synapses is established by an augmented response of AMPA receptors. The selective, strong reduction of somatic AMPA receptor currents in GluR-A–deficient mice

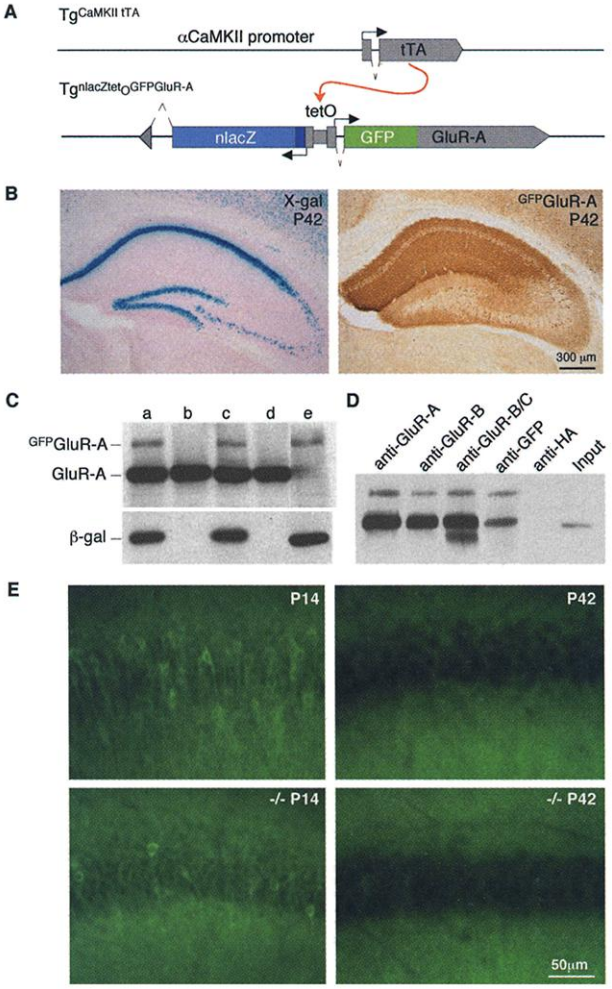

Fig. 1. GFPGluR-A expression and AMPA receptor assembly. (**A**) Schematic drawing of the αCaMKII/tTA transgene of line $Tg^{(CaMKIItTA)Mmay}$ (*17*) and the construct of line $Tg^{(nlacZtetOGFPGluR-A)A1.1}$ (*18*) for tTA-controlled expression of a nuclear β-gal and of GFPGluR-A. In the presence of dox, tTA is inactive. (**B**) Enzymatically visualized β-gal and anti-GFP–immunostained (*16*) GFPGluR-A in coronal forebrain sections of wild-type mice positive for both transgenes shown in (A). (**C**) Expression of GluR-A, GFPGluR-A, and β-gal was monitored by immunoblots of hippocampal proteins (*16*) of wild-type (b, d) and GFPGluR-A–expressing (a, c, e) mice at P14 (a, b) and P42 (c, d), and at P42 in GluR-$A^{-/-}$ mice (e). (**D**) Coimmunoprecipitations with the indicated antibodies of solubilized AMPA receptors (*19*) from brain homogenates of GFPGluR-A–expressing wild-type mice. Additionally, 5% of the homogenate (Input) used for coimmunoprecipitation was loaded. The blot was probed with anti-GluR-A. (**E**) GFPGluR-A fluorescence in CA1 neurons of wild-type and GluR-$A^{-/-}$ mice at P14 and P42.

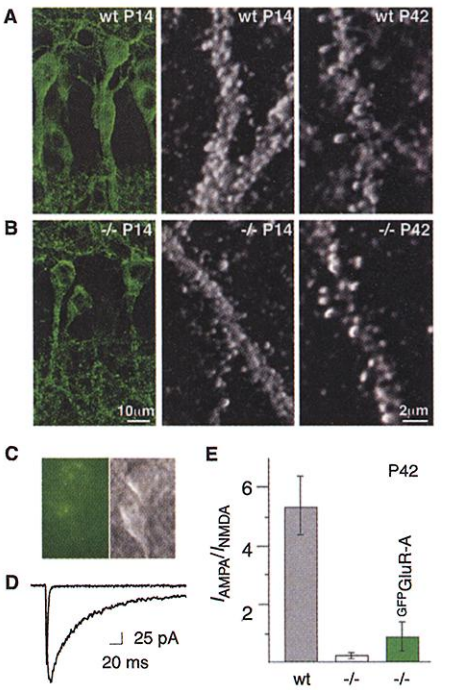

Fig. 2. GFPGluR-A in CA1 pyramidal cells: mosaic expression, spine location, and contribution to somatic AMPA currents. (**A** and **B**) Confocal images (*16*) of pyramidal cell bodies (left) and spines on dendritic shafts (middle and right) visualized by GFP fluorescence in GFPGluR-A–expressing wild-type and GluR-$A^{-/-}$ mice. At P42, for both genotypes, GFPGluR-A was dominant in spines and hardly visible in shafts. (**C**) For recordings, pyramidal cell bodies were monitored for GFPGluR-A fluorescence (left) and patched in the infrared mode (right) to determine (**D**) AMPA (fast) and NMDA (slow) receptor-mediated currents of nucleated patches (*4*). (**E**) Bar diagram depicting AMPA/NMDA current ratios in wild-type (gray, $n = 5$), GluR-$A^{-/-}$ (white, $n = 8$), and GFPGluR-A–expressing GluR-$A^{-/-}$ mice (green, $n = 7$).

(*4*) further suggests that lack of AMPA receptors at nonsynaptic sites is linked to absence of LTP. GFP-tagged AMPA receptor expression in organotypic slice cultures supports the idea that GluR-A and GluR-D subunits facilitate rapid AMPA receptor delivery in SC/CA1 synapses after LTP induction (*5*–*8*).

We now investigate the contribution of GluR-A–dependent LTP in development of hippocampal connections. We analyzed whether in adult GluR-A–deficient mice, synaptic plasticity can be restored by controlled expression of GluR-A. First, we generated mice with regulated GFPGluR-A expression and characterized the function of the fluorescent subunit in the genetic background of wild-type mice. In a second step, the GFPGluR-A expression system was transferred to GluR-$A^{-/-}$ mice, and the restoration of synaptic plasticity was studied in the presence and absence of GFPGluR-A.

Regulated GFPGluR-A expression (Fig. 1A) by the doxycycline (dox) system (*9*) provided strong GFPGluR-A immunoreactivity to the hippocampal formation at postnatal day 14 (P14) and P42 (Fig. 1B and Web fig. 1B). However, the somata of hippocampal pyramidal cells displayed different GFPGluR-A labeling intensities, indicating variable amounts of GFPGluR-A in distinct pyramidal cells (Web fig. 1C). As estimated by immunoblots (Fig. 1C), the GFPGluR-A levels were about 10% of total GluR-A, which showed that GFPGluR-A–expressing mice should not be compromised by overexpression of AMPA receptors. GFPGluR-A was incorporated in active receptor channels as evidenced by current-voltage relations (Web fig. 1A) and could be copurified with GluR-B and GluR-C from hippocampi of GFPGluR-A–expressing mice (Fig. 1D). GFPGluR-A was also associated with endogenous GluR-A (Fig. 1D), a clear indication of AMPA receptor populations with more than a single GluR-A subunit.

The trafficking of the GFPAMPA receptors seemed undisturbed because the distribution of green fluorescence mimicked the development-dependent redistribution of the AMPA receptors from somato/dendritic to dendritic location in hippocampal CA1 neurons (*10*). At P14, principal neurons in CA1 were labeled in somata and in dendritic fields, whereas at P42, somatic GFPGluR-A fluorescence disappeared (Fig. 1E). Expression levels of the transgene in the hippocampus measured by immunoblots and β-galactosidase (β-gal) activity did not change from P14 to P42 (Fig. 1C, Web fig. 1C). However, within CA1 dendrites, GFPGluR-A could be observed in spines and shafts in young animals (Fig. 2A), whereas in older mice (P42) it was difficult to find GFPGluR-A in dendritic shafts (Fig. 2A). This indicates that in adult mice, the majority of GluR-A–containing AMPA receptors is located in spines. The age-dependent difference in the GluR-A distribution pattern was not simply caused by a different amount of AMPA receptors. When AMPA receptor expression was reduced by

Departments of [1]Molecular Neurobiology and [2]Cell Physiology at the Max-Planck-Institute for Medical Research, D-69120 Heidelberg, Germany. [3]Department of Physiology, Institute of Basic Medical Sciences, University of Oslo, 0462 Oslo, Norway.

*Present address: Department of Neurophysiology, Faculty of Biology, Vrije University, 1081 HV, Amsterdam, Netherlands.

†To whom correspondence should be addressed. E-mail: sprengel@mpimf-heidelberg.mpg.de

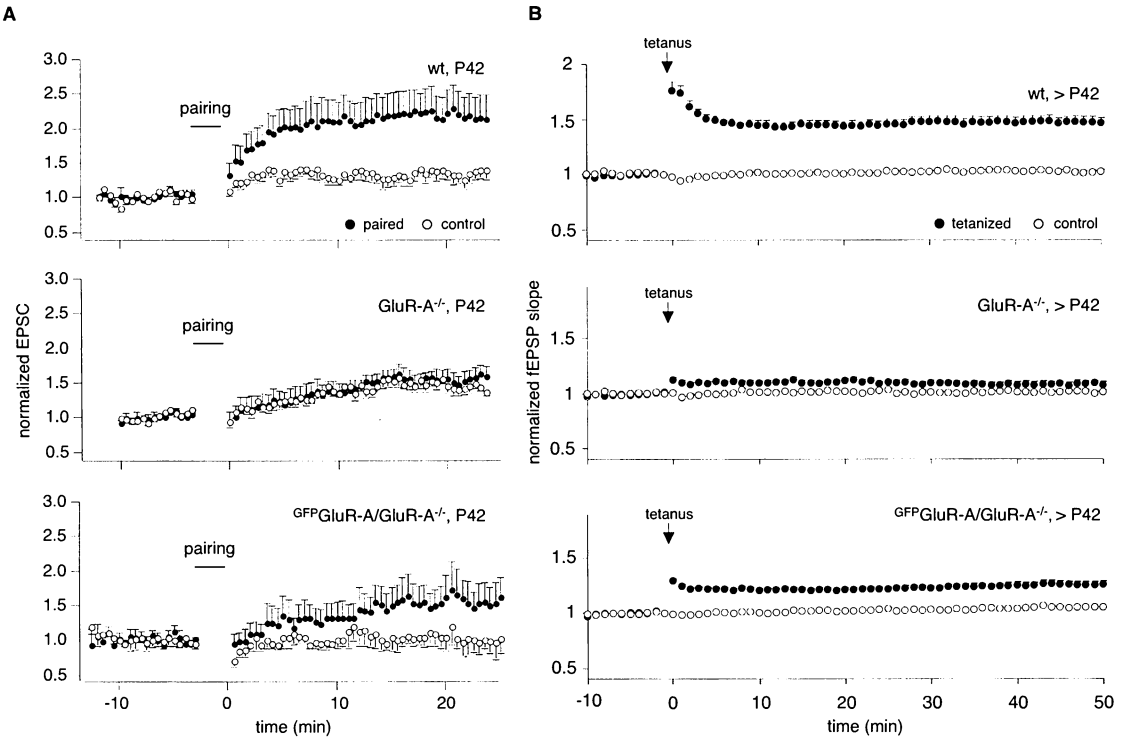

Fig. 3. Recovery of SC/CA1 LTP in ^{GFP}GluR-A–expressing GluR-A$^{-/-}$ mice. (**A**) Summary graphs of SC-evoked EPSC amplitudes in the paired (filled circles) and unpaired control pathway (open circles) before and after pairing in CA1 pyramidal cells of wild-type (top, n = 7), GluR-A$^{-/-}$ (middle, n = 5), and ^{GFP}GluR-A–epressing GluR-A$^{-/-}$ mice (bottom, n = 5 GFP fluorescent cells) (*12*). (**B**) Summary graphs of extracellular fEPSP slopes evoked in the tetanized (closed circles) and untetanized (open circles) pathways (*4*) in slices of wild-type (top, n = 35), GluR-A$^{-/-}$ (middle, n = 34), and ^{GFP}GluR-A–expressing GluR-A$^{-/-}$ mice (bottom, n = 21). Data were obtained in Ringer's solution containing 2 mM Ca^{2+} and 2 mM Mg^{2+}. The LTP level of ^{GFP}GluR-A–expressing GluR-A$^{-/-}$ mice differed significantly from LTP of GluR-A$^{-/-}$ (P = 0.0001) and wild-type (P = 0.004) mice. In all genotypes, the untetanized control pathway showed no improved response (102 ± 2%, 103 ± 1%, and 104 ± 1%). Vertical bars indicate SEM.

transfer of the ^{GFP}GluR-A expression system into the genetic background of GluR-A–deficient mice, we observed a ^{GFP}GluR-A fluorescence pattern that was very similar to that detected in the wild-type background (Fig. 2B).

We next investigated if the ^{GFP}GluR-A subunit was able to replace the function of the depleted endogenous GluR-A in GluR-A–deficient mice. Nucleated patch recordings from fluorescent CA1 pyramidal cells (Fig. 2, C through E) of ^{GFP}GluR-A–expressing GluR-A$^{-/-}$ mice showed a relatively small increase in the AMPA/*N*-methyl-D-aspartate (NMDA) receptor current ratio (0.92 ± 0.51) over that of GluR-A–deficient mice (0.27 ± 0.12). However, the current ratio remained far below that determined in wild-type mice (5.41 ± 1.01). This result is in agreement with immunological data, which suggested that in the mosaic CA1 cell population the strongest ^{GFP}GluR-A–expressing cells have less ^{GFP}GluR-A than endogenous GluR-A. Despite the low AMPA receptor–mediated soma currents, pathway specific cellular LTP induced by pairing (*11, 12*) was evoked in ^{GFP}GluR-A positive CA1 neurons and was not detectable in CA1 cells of GluR-A–deficient mice at P42 (Fig. 3A). The mosaic ^{GFP}GluR-A expression in the CA1 cell population (Fig. 2, A and B) caused partial recovery of field LTP (Fig. 3B). The average field excitatory postsynaptic potential (fEPSP) slope 40 to 45 min after tetanization (100 Hz, 1 s) in adult ^{GFP}GluR-A–expressing

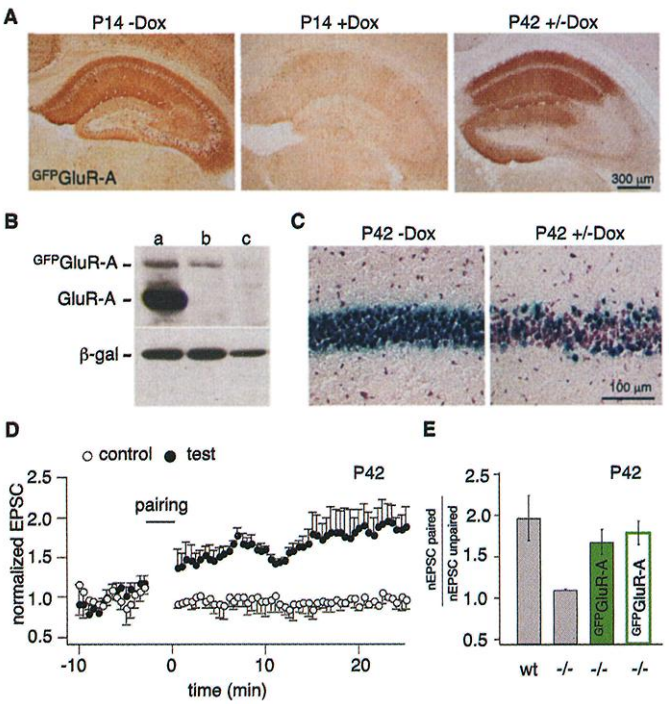

Fig. 4. Rescue of LTP in GluR-A–deficient mice by delayed ^{GFP}GluR-A expression induced at P21 and analyzed at P42. (**A**) GFP immunoreactivity seen in the hippocampus of P14 ^{GFP}GluR-A–expressing mice (left) was not detected in mice nursed under dox (75 µg/ml drinking water) (middle) (*16*). When dox was removed at P21, GFP immunoreactivity was observed at P42 (right). (**B**) From immunoblots, ^{GFP}GluR-A (upper blot) and β-gal expression (lower blot) at P42 was high in hippocampi of ^{GFP}GluR-A–expressing wild-type (a) and GluR-A$^{-/-}$ kept without dox (b), but lower in GluR-A$^{-/-}$ mice when dox was removed at P21 (c). (**C**) Cryostat sections showing that at P42 the number of blue, β-gal–positive CA1 pyramidal cells was higher (left) compared to mice with delayed ^{GFP}GluR-A and β-gal expression induced at P21 (right) (*20*). (**D**) Summary graphs of SC-evoked EPSC amplitudes as described in Fig. 3A, but now analyzed in CA1 cells of ^{GFP}GluR-A–expressing GluR-A$^{-/-}$ mice nursed under dox until P21 (n = 3 fluorescent cells). (**E**) Twenty minutes after pairing, the averaged normalized EPSC amplitudes are significantly increased in paired versus control pathway of wild-type (n = 8) and GluR-A$^{-/-}$ mice with constitutive (n = 8; green) or P21-induced ^{GFP}GluR-A expression (n = 6; green/white) and unchanged in GluR-A–deficient mice (n = 7). The LTP level in GluR-A$^{-/-}$ mice with constitutive or P21-induced ^{GFP}GluR-A differed significantly from LTP in in GluR-A$^{-/-}$ mice (P = 0.002 and P = 0.0006, respectively), whereas they did not differ significantly from each other (P = 0.59) nor from that in wild-type mice (P = 0.34 and P = 0.59, respectively).

GluR-A$^{-/-}$ mice was 125 ± 3%, clearly between that of adult GluR-A–deficient (108 ± 3%) and wild-type (147 ± 5%) mice.

A continued developmental expression of GluR-A–mediated synaptic plasticity might be important for the establishment of LTP in synapses of adult animals. We determined whether "delayed" expression of GluR-A—i.e., expression only in the adult brain—can restore LTP in hippocampal SC/CA1 connections of GluR-A$^{-/-}$ mice. For expression delay, transcription of the ^{GFP}GluR-A transgene was switched off by dox until P21. Figure 4A and Web fig. 1D illustrate that in the continued presence of dox, neither ^{GFP}GluR-A nor β-gal was detected at P14. When dox was removed at P21, ^{GFP}GluR-A and β-gal expression was induced, and both proteins were readily expressed in CA1 at P42. The delayed induced expression of ^{GFP}GluR-A and β-gal did not reach the levels seen in mice that had both genes activated during development (Fig. 4B). We estimate that the level of hippocampal ^{GFP}GluR-A was, at most, 20% of that in mice raised without dox. The decreased delayed expression was accompanied by a reduced number of β-gal–positive cells in CA1 (Fig. 4C). In acute slices, we identified by fluorescence CA1 pyramidals that expressed ^{GFP}GluR-A and determined cellular LTP. In neurons with ^{GFP}GluR-A, cellular LTP was expressed (Fig. 4, D and E). The averaged normalized excitatory postsynaptic current (EPSC) amplitudes 20 min after pairing were 1.67 ± 0.15 in GluR-A–deficient, constitutively ^{GFP}GluR-A–expressing mice and 1.78 ± 0.14 after ^{GFP}GluR-A induction. Wild-type and GluR-A$^{-/-}$ mice had normalized EPSC amplitudes of 1.96 ± 0.27 and 1.09 ± 0.07, respectively.

In adult GluR-A–deficient mice, the lack of LTP induced at SC/CA1 synapses by pairing or tetanic stimulation could be restored by the expression of ^{GFP}GluR-A. This supports a strict GluR-A dependence of rapidly increased synaptic efficacy in both protocols of LTP induction. At the cellular level, LTP was rescued to its full extent, although the expression of ^{GFP}GluR-A did not reach wild-type levels. Somatic AMPA receptor current amplitudes were still limited to about 10% of those of wild-type mice, indicating that an AMPA receptor density generating only 10% of extrasynaptic currents was sufficient for expression of potentiation.

In GluR-A–deficient mice, functional synaptic SC/CA1 connections were formed in the absence of GluR-A and GluR-A–dependent plasticity. Synapses were made modifiable when the block of ^{GFP}GluR-A gene expression was unlocked by removing dox, and ^{GFP}GluR-A was readily synthesized and incorporated into dendritic spines. This implies that mature synapses were prebuilt for GluR-A–mediated potentiation even when GluR-A was never expressed. It is possible that in wild-type mice early in development, other GluR subunits (GluR-C and GluR-D) contribute to AMPA receptor dependent plasticity and that in mature synapses, one of these subunits is replaced by GluR-A. The GluR-D subunit is discussed as being important for neonatal plasticity (*5*). However, the mechanism of activity-induced AMPA receptor delivery to the synapse differs for GluR-D- and GluR-A–containing receptors (*8*). Therefore, other mechanisms of neuronal plasticity are more likely to establish functional hippocampal circuitry. Recently, we found a GluR-A–independent form of LTP in juvenile mice that might be important for the regular development of hippocampal connections (*10*). The fact that the induction and establishment of LTP in adult mice can be repressed or restored shows that regulated expression of individual AMPA receptor subunits, especially of GluR-A, can substantially alter the functional properties of hippocampal synaptic connections, in particular their ability to undergo long-term changes in synpatic efficacy.

References and Notes

1. K. Keinänen *et al.*, *Science* **249**, 556 (1990).
2. M. Hollmann, S. Heinemann, *Annu. Rev. Neurosci.* **17**, 31 (1994).
3. R. Dingledine, K. Borges, D. Bowie, S. F. Traynelis, *Pharmacol. Rev.* **51**, 7 (1999).
4. D. Zamanillo *et al.*, *Science* **284**, 1805 (1999).
5. J. J. Zhu, J. A. Esteban, Y. Hayashi, R. Malinow, *Nature Neurosci.* **3**, 1098 (2000).
6. S. H. Shi *et al.*, *Science* **284**, 1811 (1999).
7. Y. Hayashi, S. H. Shi, J. A. Esteban, A. Piccini, J. C. Poncer, R. Malinow, *Science* **287**, 2262 (2000).
8. R. Malinow, Z. F. Mainen, Y. Hayashi, *Curr. Opin. Neurobiol.* **10**, 352 (2000).
9. M. Gossen, A. L. Bonin, S. Freundlieb, H. Bujard, *Curr. Opin. Biotechnol.* **5**, 516 (1994).
10. V. Jensen *et al.*, unpublished data.
11. H. X. Chen, N. Otmakhov, J. Lisman, *J. Neurophysiol.* **82**, 526 (1999).
12. Whole-cell voltage clamp recordings were made from CA1 pyramidal cells in 250-μm slices under visual control (*4*). For LTP measurements, EPSCs were evoked every 5 s by SC stimulation from two independent inputs (*10*), one of which was paired and the other of which was used as a control, with two patch pipettes used as stimulating electrodes. All measurements were at –70 mV membrane potential. LTP was evoked and recorded according to (*11*) by voltage-clamping the membrane potential of the postsynaptic pyramidal cell to 0 mV and stimulating the test pathway every 1.5 s for 3 min. Extracellular bath solution: 124 mM NaCl, 2.5 mM KCl, 10 mM glucose, 26 mM $NaHCO_3$, 1.25 mM NaH_2PO_4, 4 mM $CaCl_2$, 4 mM $MgSO_4$, 20 μM bicuculline, and 10 μM glycine (pH 7.2). Recording pipettes were filled with 120 mM Cs gluconate, 10 mM CsCl, 8 mM NaCl, 2 mM Mg-ATP, 10 mM phosphocreatine, 0.3 mM GTP, 0.2 mM EGTA, and 10 mM Hepes (pH 7.3) (295 mOsm). Data are mean ± SEM unless otherwise stated, and the statistical significance levels were calculated from a two-tailed *t* test.
13. S. A. Petersen, R. D. Fetter, J. N. Noordermeer, C. S. Goodman, A. DiAntonio, *Neuron* **19**, 1237 (1997).
14. S. Zolotukhin, M. Potter, W. W. Hauswirth, J. Guy, N. Muzyczka, *J. Virol.* **70**, 4646 (1996).
15. U. Baron, S. Freundlieb, M. Gossen, H. Bujard, *Nucleic Acids Res.* **23**, 3605 (1995).
16. H. E. Krestel, M. Mayford, P. H. Seeburg, R. Sprengel, *Nucleic Acids Res.* **29**, e39 (2001).
17. M. Mayford, M. E. Bach, Y. Y. Huang, L. Wang, R. D. Hawkins, E. R. Kandel, *Science* **274**, 1678 (1996).
18. For myc-GFP–tagged GluR-A, the signal sequence of CP3 (*13*) followed by the epitope c-myc was inserted in frame to GFP (*14*). The myc-GFP gene was then inserted after the putative signal sequence of rat GluR-A. The myc–GFP–GluR-A (^{GFP}GluR-A) was subcloned into modified pBI-1 (*15*) to provide pnlacZ/^{GFP}GluR-A. It was used to generate transgenic mice, and founders were identified by PCR (polymerase chain reaction) of tail DNA (*16*) using primer GluR-A–VM4 (CTCTCTGCAGGACTGACAGG) and VM4 (CTCCCAGACAACCATTACCTGTCC) to amplify a 565–base pair fragment.
19. Hippocampi homogenates (*16*) were cleared by centrifugation (5 min at 1000*g*) and were mixed 1:1 with 25 mM Hepes, 300 mM NaCl, and 2% Triton X-100 (pH 7.4), containing protease inhibitors. After 30 min at 4°C and centrifugation (10 min at 10,000*g*), the supernatant was used for immunoprecipitation (IP). Each IP (400 μl) at a protein concentration of 0.75 μg/μl was incubated with the appropriate antibodies (2 μg anti-GluR1, 2 μg anti-GluR2, 2 μg anti-GluR2/3, 4 μg anti-GFP, 2 μg anti-HA) overnight at 4°C. IPs were collected on protein A agarose, and proteins were eluted in 2× SDS buffer. For each precipitation, proteins were resolved on a 7% SDS-polyacrylamide gel, transferred on nitrocellulose membranes and probed with anti-GluR-1.
20. Coronal 15-μm cryostat sections of frozen brains were mounted on cover slips, postfixed for 5 min in phosphate-buffered saline (PBS) and 2% paraformaldehyde, and rinsed with PBS. Sections were stained for β-gal activity (*16*), washed twice in PBS and once in water, counterstained with red neutral (1%) in 50 mM sodium acetate (pH 3.3), and dehydrated three times in ethanol [70, 90, 99.5% (v/v)]. Dried sections were embedded in Eukitt.

21. We thank H. Bujard for his interest and support with the tet system; F. Zimmermann, G. Giese and A. Herold for technical assistance; M. Mayford for KT-1 mice; and N. Muzyczka for GFP cDNA. This work was supported in part by Deutsche Forschungsgemeinschaft SFB Grant 317 (R.S.), Volkswagen-Stiftung (R.S., B.S., P.H.S), and European Union 5th Framework Grant QLG3-CT-1999-01022.

29 January 2001; accepted 16 May 2001